

Fabrication of PLA-HAp-CS Based Biocompatible and Biodegradable Feedstock Filament Using Twin Screw Extrusion



Nishant Ranjan, Rupinder Singh, I. P. S Ahuja, and Jatenderpal Singh

1 Introduction

FDM deals with additive manufacturing (AM) rule of setting out the material in type of layers/cuts on a fixtureless stage [1–3]. There are few distinct strategies for 3D printing; however, the most generally utilized is a procedure known as FDM. The FDM printers utilize a thermoplastic fiber, which is warmed to its dissolving point and afterward expelled, layer by layer, to make a three dimensional product [4]. FDM is one of the AM processes that build a part of any geometry by ordered deposition of polymeric material in form of feed stock filament on a layer-by-layer basis. The method uses heated thermoplastic filaments which square measure extruded from the tip of the nozzle in an exceedingly prescribed manner in an exceedingly semi-molten state and solidify at chamber temperature. The properties of engineered elements depend upon the setting of various method parameters mounted at the time of fabrication [5]. Feedstock filament is one of the mostly effected input parameters for 3D printing by using FDM [6].

Bone repair or recovery is a typical yet entangled clinical issue in orthopaedic surgery. Despite the fact that autografts what is more, allografts have been generally

N. Ranjan

Department of Production Engineering, Guru Nanak Dev Engineering College, Ludhiana, Punjab, India

Department of Mechanical Engineering, Punjabi University, Patiala, Punjab, India

R. Singh (✉)

Department of Production Engineering, Guru Nanak Dev Engineering College, Ludhiana, Punjab, India

I. P. S Ahuja

Department of Mechanical Engineering, Punjabi University, Patiala, Punjab, India

J. Singh

Department of Defence Production, DGQA, SQAE (A), Jabalpur (M.P), India

utilized as a part of clinical treatment and look into, they both have particular issues. Autografts require auxiliary surgery to get give bone from the patient's claim body; however the measure of contributor bone is constrained [7, 8]. Bone tissue engineering substitutes are another alternative for treating bone imperfections, and have been proclaimed as an elective system to recover bone [9]. The improvement of biomimetic materials has for some time been a noteworthy objective in the field of bone tissue engineering. Natural bone is a complex organic-inorganic nano-composite material, in which HAp nano-crystallites and collagen fibers are efficient in a various levelled engineering more than a few length scales [10, 11]. Normal polymers and their subordinates have been progressively utilized as a contrasting option to synthetic polymers due to their biodegradability and organic action [12–15]. The CS, a characteristic biodegradable polymer, is a low acetyl substituted type of chitin. Inferable from its one of kind properties, including biodegradability, non-poisonous quality, antibacterial impact and bio-similarity, much consideration has been paid to CS-based biomedical materials [16–19]. However, the absence of bone-bonding bioactivity, low mechanical properties and extricating of auxiliary respectability under wet conditions constrain its utilization in bone tissue building. In this way, it is attractive to build up a composite material with the positive properties of both CS and HAp. The outlined composites are relied upon to indicate expanded osteo-conductivity and biodegradation together with adequate mechanical properties, which will be of incredible significance for bone renovating [20–22]. It has been accounted for that Hap and CS composites indicate best biocompatibility and good holding capacity with encompassing host tissues inalienable from HAp [23, 24]. It has additionally been demonstrated that HAp and CS composites can additionally upgrade tissue regenerative adequacy and osteo-conductivity. The methodologies as of now used to get HAp composite materials depend on mechanical blending, co-precipitation [25, 26].

PLA is a nontoxic, biodegradable material with high mechanical strength that is generally utilized as a part of surgery [27–32]. With a specific end goal to build the mechanical quality of CS-HAp composite platforms; in this study effort has been made to use PLA into the CS-HAp framework. An advantage of PLA-based biomaterials has been their ability to be fabricated into a variety of structures with the appropriate mechanical properties, topography, geometry, and architecture as required for diverse biomedical applications. One of the oldest methods to fabricate PLA based products has been fiber-spinning from either polymer solution or melt. As PLA is soluble in a wide array of solvents, solution spinning processes has also been widely utilized to fabricate fibers for biomedical applications [33]. Historically, mono and multi filament sutures have been prepared from PLA-based fibers by spinning; but due to their longer degradation times, other aliphatic polyesters such as poly-glycolic acid (PGA) have now replaced PLA [34]. In addition, woven, knitted, and braided structures produced from spun fibers have found orthopedic applications in bone, ligament, and cartilage regeneration [35, 36]. Further the HAp has stoichiometric Ca/P ratio of 1.67, which is identical to bone apatite [37–41], hence PLA reinforced with Hap can be one of the solution for human implants. But hitherto very less has been reported for preparation of in-house biocompatible and

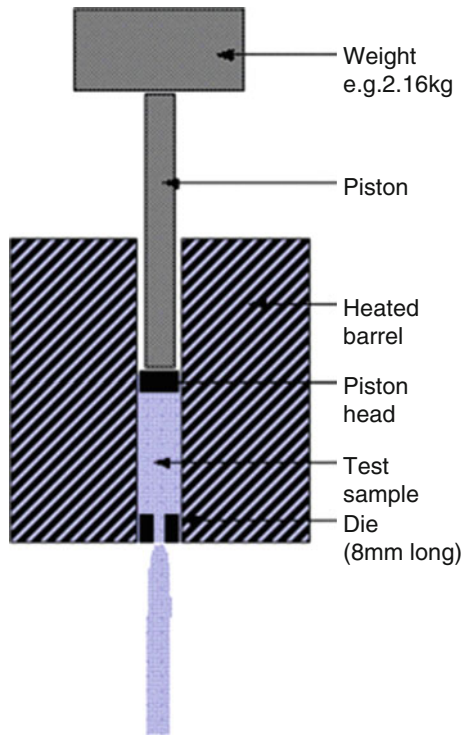
biodegradable feedstock filament comprising of PLA reinforced with CS, HAP for commercial FDM setup. In this study rheological, tensile, thermal and microscopic properties have been ascertained and regression model has been developed to determine the best setting of TSE for drawing the feedstock filament for further printing of functional prototypes. These functional prototypes will act as osteo-conductive and osteo-inductive osteo-allograft by providing attractive surface for new bone cells (osteoblasts).

2 Melt Flow Index

Melt flow index (MFI) of any thermoplastic material is defines as a deposition in g/10 min through melt flow tester at certain standard temperature i.e. 210 degree centigrade. The MFI is a determination of glass transition temperature as well as flow-ability of the thermoplastic materials. This is a well-known melting property of thermoplastic material checked by equipment called melt flow tester. Figure 1 shows a schematic of melt flow tester.

The above shown construction (Fig. 1) of melt flow tester is consist of cylindrical barrel which is wrapped and surrounded by a heater coil, heater have an outer

Fig. 1 Basic construction of melt flow tester



periphery of insulation material to restrict the losses of heat and this heater is controlled automatically by process control box. This set-up is also consisting of a standard weight applied through the piston, a piston head and dies to deposit the materials.

2.1 Procedure to Determine Melt Flow Index

- To determine MFI of certain composition, mixture is poured to the cylinder and a temperature condition is to be set.
- Then left the machine sometime to achieve the predefined temperature.
- After establishing a predefined temperature, pressure is applied with the piston bar into the cylinder by certain weight (according to ASTM D1238) above to the piston bar.
- After placement of plunger, melted plastic come out of the barrel.
- When the time cycle on the digital timer completes, the cutter will automatically cut the sample from the barrel.
- Weigh the melted sample using a digital balance. This weight will be used for calculating the MFI of the sample.

Formula to calculate MFI:-

$$\text{MFI} = \text{Weight of sample in g}/10 \text{ min.}$$

3 Extrusion

Extrusion is a manufacturing process in which metal or plastic materials are forced/pushed through a fixed cross-sectional profile or die to produce a continuous ribbon of the formed product or, Extrusion is a manufacturing process in which raw materials (plastic/metal) are melted and made into continual profile.

Extrusion process is starting by feeding of material (plastic/metal) in the form of granules, pellets, powders or flakes from a hopper into the zone of barrel of the extruder. After that, materials are gradually melting by heat, which was produced by the mechanical energy (generating by screw turning) and by the heaters which is positioned along the barrel. The molten materials (plastic/metal) are pushed/forced into a die, which structure the materials into a pipe hard during cooling process. Figure 2 shows cross-section view of single and TSE.

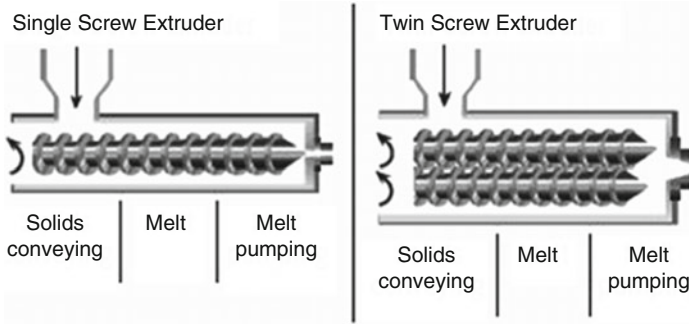


Fig. 2 Cross-section view of single and twin-screw extruder

3.1 *Twin Screw Extrusion*

TSE is used extensively for mixing, compounding or reacting polymeric materials. The flexibility of TSE equipment allows this operation to be designed specifically for the formulation being processed. For example, the two screw may be co-rotating or counter-rotating, intermeshing or non-intermeshing. In addition, the configurations of the screws themselves may be varied using forward conveying elements, reverse conveying elements, kneading blocks, and other designs in order to achieve particular mixing characteristics. In the TSE process, the raw materials may be solids (granules, powders & flours), slurries, liquids, and possibly gases.

4 Fused Deposition Modeling (FDM)

FDM is an AM technology commonly used for modeling, prototyping, and production applications.

4.1 *The Technology*

The FDM process constructs three-dimensional objects directly from 3D CAD data. A temperature-controlled head extrudes thermoplastic material layer by layer.

The FDM process starts with importing an STL file of a model into a pre-processing software. This model is oriented and mathematically sliced into horizontal layers varying from ± 0.127 to 0.254 mm thickness. A support structure is created where needed, based on the part's position and geometry. After reviewing the path data and generating the tool-paths, the data is downloaded to the FDM machine. The system operates in X, Y and Z axes, drawing the model one layer at a time. This process is similar to how a hot glue gun extrudes melted beads of glue. The temperature-controlled extrusion head is fed with thermoplastic modeling

material that is heated to a semi-liquid state. The head extrudes and directs the material with precision in ultrathin layers onto a fixtureless base. The result of the solidified material laminating to the preceding layer is a plastic 3D model built up one strand at a time. Once the part is completed the support columns are removed and the surface is finished.

4.2 Process

FDM begins with a software process, developed by Stratasys, which processes an STL file (stereo-lithography file format) in minutes, mathematically slicing and orienting the model for the build process. If required, support structures are automatically generated. The machine dispenses two materials – one for the model and one for a disposable support structure. The thermoplastics are liquefied and deposited by an extrusion head, which follows a tool-path defined by the CAD file. The materials are deposited in layers as fine as 0.04 mm (0.0016”) thick, and the part is built from the bottom up – one layer at a time. FDM works on an “additive” principle by laying down material in layers. A plastic filament or metal wire is unwound from a coil and supplies material to an extrusion nozzle which can turn the flow on and off. The nozzle is heated to melt the material and can be moved in both horizontal and vertical directions by a numerically controlled mechanism, directly controlled by a computer-aided manufacturing(CAM) software package. The model or part is produced by extruding small beads of thermoplastic material to form layers as the material hardens immediately after extrusion from the nozzle. Stepper motors or servo-motor are typically employed to move the extrusion head. Several materials are available with different trade-offs between strength and temperature properties. FDM setup shows in Fig. 3.

A “water-soluble” material can be used for making temporary supports while manufacturing is in progress, this soluble support material is quickly dissolved with specialized mechanical agitation equipment utilizing a precisely heated sodium hydroxide solution.

5 Differential Scanning Calorimetry (DSC)

5.1 Technique

DSC is used to measure melting temperature, heat of fusion, latent heat of melting, reaction energy and temperature, glass transition temperature, crystalline phase transition temperature and energy, precipitation energy and temperature, de-naturization temperatures, oxidation induction times, and specific heat or heat capacity. DSC measures the amount of energy absorbed or released by a sample when it is heated or cooled, providing quantitative and qualitative data on endothermic (heat absorption) and exothermic (heat evolution) processes.

Fig. 3 Fused deposition modeling process

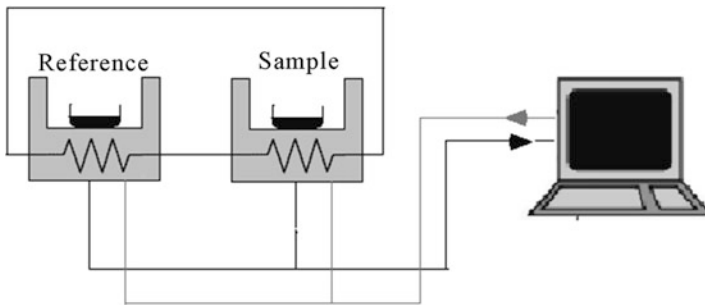
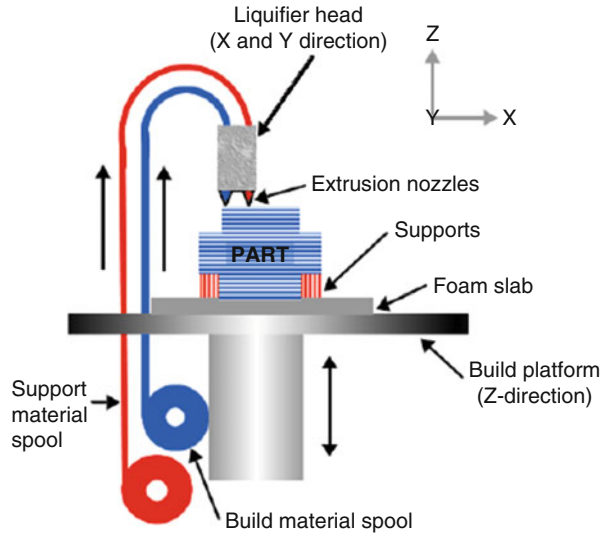


Fig. 4 Schematic of METTLER TOLEDO DSC

The sample is placed in a suitable pan and sits upon a constantan disc on a platform in the DSC cell with a chromel wafer immediately underneath. A chromel-alumel thermocouple under the constantan disc measures the sample temperature. An empty reference pan sits on a symmetric platform with its own underlying chromel wafer and chromel-alumel thermocouple. Heat flow is measured by comparing the difference in temperature across the sample and the reference chromel wafers. Pans of Al, Cu, Au, Pt, alumina, and graphite are available and need to be chosen to avoid reactions with samples. Figure 4 shows schematic of commercial METTLER TOLEDO DSC.

Atmospheres Nitrogen, air, oxygen, argon, vacuum, controlled mixed gases.

6 Materials and It's Prepration

6.1 Materials

An injection grade of PLA is available from commercial manufacturer, Nature Works (United State), Ingeo™ 3052D, density 1.24 g/cm³, melting temperature 173–178 °C, glass transition temperature 55–60 °C, melt flow rate 14 g/10 min (at 210 °C, 2.16 Kg) has been selected as a polymer matrix [42] was bought from Nature Works, Chennai. Chitosan (CS, degree of deacetylation >90%), HAp (colorless & brittle) (Size:- 20–100 μm) available from local manufacturer at Ludhiana (India) has been used in this study.

6.1.1 Preparation of Materials (PLA, HAp and CS)

PLA pellets were pre-dried at 80 °C in a vacuum oven overnight (8–10 h), while HAp powder and CS were dried at 40 °C for 2 h [43, 44] in vacuum oven so as to remove moisture content. The mixtures of various proportions were added with 2–3 ml of coconut oil and mixed using ball mill at 40 rpm for 4 h.

7 Preparation of Feed Stock Filament On TSE for FDM

In pilot experimentation, an effort has been made to prepare the feed stock filament of biocompatible/biodegradable grade of PLA. The first step was to check the possibility of preparation of feed stock filament of PLA reinforced with HAp and CS with varying input parameters. Taking random selection of different composition/ proportions of polymer materials and fillers first check the flowability after that thermal, tensile and microscopic test are to be done. Suitable composition of PLA-HAp-CS for fabrication of feed stock filament on TSE and also making of scaffolds on FDM are to be selected. The feed stock filament has been prepared as per Taguchi L9 (3³) orthogonal array. For this study commercial, make: HAAKE Mini CTW, Germany has been used.

7.1 Rheological Behavior

The feasibility to ascertain the fabrication of feedstock filament of PLA-HAp-CS of varying proportion started with pilot experimentation to access Melt Flow Index (MFI) in accordance with ASTM-D1238. The mixtures of various proportions were added with 2–3 ml of coconut oil and mixed using ball mill at 40 rpm for 4 h. Table 1 show the different composition of PLA-HAp-CS (by weight %age) MFI (g/10 min).

Table 1 Melt flow index results

S. No.	Proportions (PLA-HAp-CS) (by weight %)	Observed MFI (g/10 min)	Flow from nozzle	Remarks
1	100-0-0	13.52	Continuous	Satisfactory
2	84-4-12	10.512	Continuous	Satisfactory
3	80-8-12	9.015	Continuous	Satisfactory
4	76-12-12	3.125	Discontinuous	Not Satisfactory
5	91-8-1	12.352	Continuous	Satisfactory
6	90-8-2	11.575	Continuous	Satisfactory
7	89-8-3	7.474	Discontinuous	Not Satisfactory
8	88-8-4	4.465	Discontinuous	Not Satisfactory

Table 2 Results of fabricated feed stock filament on TSE

S. No	Composition	Output parameters		
		Flow continuity	Average outside diameter (mm)	Peak strength (MPa)
1	84-4-12	Yes	1.85	2.10
2	80-8-12	Yes	1.78	2.43
3	91-8-1	Yes	1.86	3.27
4	90-8-2	Yes	1.87	3.23

As observed from Table 1 the composition/proportion at S. No. 2 (84-4-12), 3 (80-8-12), 5 (91-8-1) and 6 (90-8-2) were selected for further fabrication of feed stock filament. The remaining compositions were not selected, as the flow was not continuous. Sample 1 has been not selected because of in this composition no fillers are to be reinforced. The four compositions/proportions of PLA-HAp-CS as derived from MFI test were extruded on the TSE.

7.2 Tensile Behavior

Four compositions/proportions of PLA-HAp-CS, which derived from MFI tester, are to be drawn by TSE, make: HAAKE Mini CTW, Germany has been used. As shown in Table 2, different combinations of input factors were tried during pilot study. The successful results arrived from the experimentations are listed in Table 2.

According to Table 2, flow continuity of all four compositions/proportions were found suitable and it is expected that the filament will not break at the time of part printing. The experiment was repeated three times in order to reduce the experimental error. It has been observed that peak strength of 91-8-1 and 90-8-2 are maximum and very close to each other while remaining compositions/ proportions have lower

peak strength. According to Table 2, it has been concluded that for fabrication of biocompatible/biodegradable feedstock filament best suitable compositions are 91-8-1 and 90-8-2.

7.3 Thermal Behavior

Thermal behaviour of the material is one of the major constraints for the use of developed filament in clinical dentistry. For thermal testing of the material in the present study DSC has been used. DSC comprises of glass transition, melting point, enthalpy change, and decomposition of the material with respect to the rising of temperature. Common usage includes investigation, selection, comparison and end-use performance evaluation of materials in research, quality control and production applications.

For thermal analysis METTLER TOLEDO, Model DSC3, Swiss make with STAR^e (SW 14.00) software was used in N₂ gas environment. The typical DSC setup determines the behaviour of applied samples by taking references from standard sample, both enclosed in a metallic crucible (Al or platinum). As shown in Fig. 5, DSC sensor uses two crucibles for heating and cooling, one for reference and another for sample.

As shown in Fig. 6, for thermal analysis three heating-cooling cycles are involved. In first cycle, initially heat the sample with comparison to reference from 30 °C to 220 °C at the rate of 10 K/min, after that in the presence of N₂ gas (flow rate is 50.0 ml/min) cooling process is done in which matter was cooled from 220 °C to 30 °C at the rate of 10 K/min. After that in the second and third cycle, same process was repeated. The maximum temperature is taken 220 °C because of the material was burnt near 240 °C and lower temperature is generally taken as near to room temperature.

The first cycle of the test is generally not considered for assessment as the sample may contain some foreign substances and may deviate from actual result. The average of second and third cycle was considered for final results. The same are tabulated in Table 3.

Based on Table 3, it has been observed that glass transition temperature lies between 56.5 °C and 57.37 °C, crystallinity of the compositions fall in between 1.20 and 10.50% and the melting point temperature in between 152.46 and 159.87 °C. For fabrication of feedstock filament on TSE and working on FDM glass transition temperature and melting temperature are best suitable range, but for biomedical applications/implants crystallization of material must be low. According to Table 3, it has been concluded that best composition for fabrication of feedstock filament based on crystallization are 91-8-1 and 80-8-12 for further experimentation work. Based on Thermal, Tensile and rheological behaviour it was concluded that two compositions 91-8-1 and 90-8-2 are SEM view performed for selection of best composition.

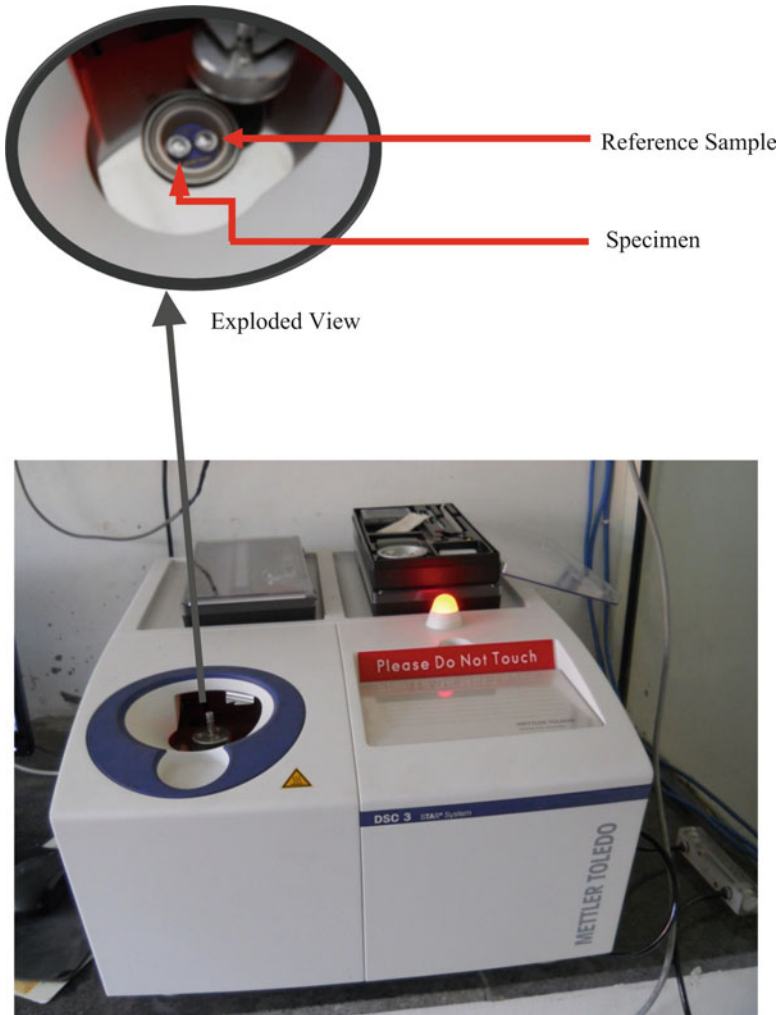


Fig. 5 Differential scanning calorimetry test

7.4 Scanning Electron Microscopic Behavior

After successful runs of feed stock filament, all samples were subject to SEM analysis (Model no. JEOL JSM-6510LV SEM, Japan) Figs. 7 and 8 shows the cross sectional view of different composition (PLA91-HAp8-CS1 & PLA90-HAp8-CS2) feedstock filament with $\times 200$ magnification, where feedstock filament was broken during the tensile testing. These images show that lots of cavities are present in the cross-section, in whole wire.

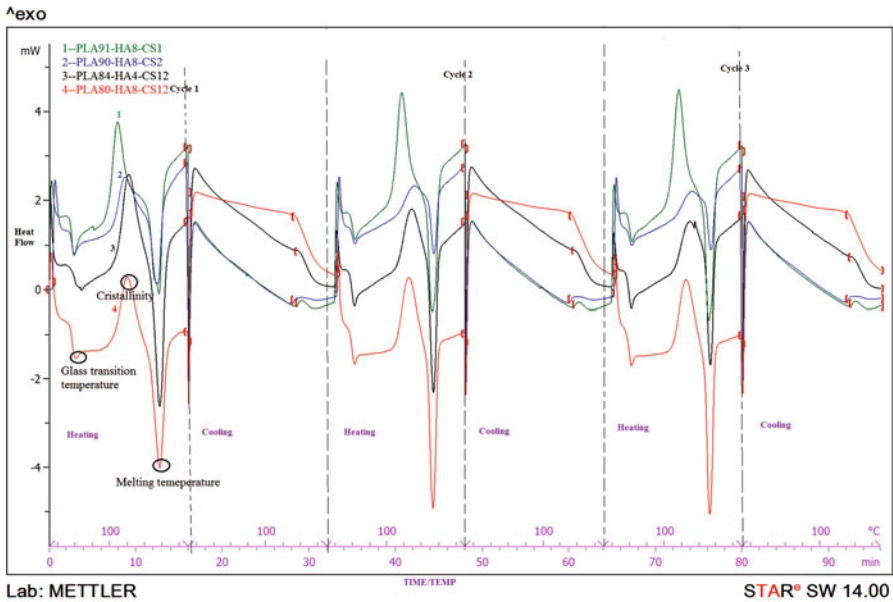


Fig. 6 Thermal analysis (DSC) curve of feed stock filament

Table 3 Thermal properties of the specimens

Compositions	Glass transition temperature (°C)	Crystallization (%)	Melting temperature (°C)
91-8-1	56.50	3.13	153.17
90-8-2	57.19	10.50	159.87
84-4-12	56.90	7.37	152.46
80-8-12	57.37	1.20	153.95

For better understanding higher magnifications images were taken. Figures 9 and 10 shows that the cross sectional view of composition PLA91-HAp8-CS1 with $\times 400$ magnification and PLA90-HAp8-CS2 with $\times 1600$ magnification. As observed from Figs. 7, 8, 9, and 10, the feedstock filament grain structure is similar to open porous structure, which is very useful for cell growth.

7.5 Design of Experiment (DOE)

The feed stock filament has been prepared as per Taguchi L9 (3^3) orthogonal array. Table 4 shows the control log of experimentation based upon Taguchi L9 (3^3) orthogonal array which was 9 runs of experimentation. A total of 9 sets of specimen

Fig. 7 Fabricated feedstock filament of composition 91-8-1($\times 200$)

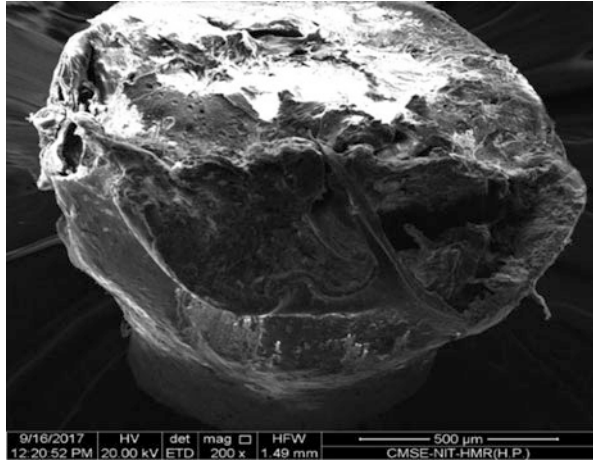
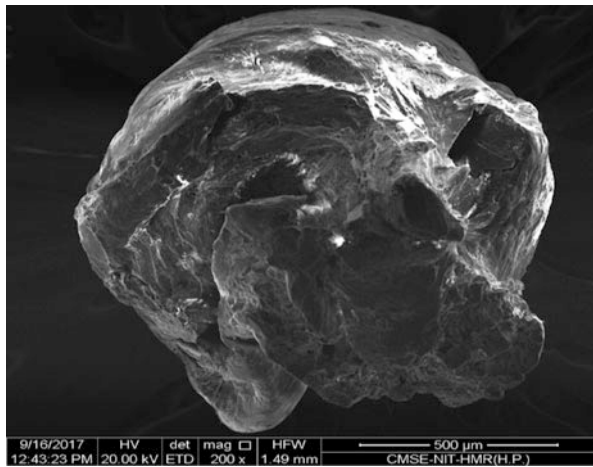


Fig. 8 Fabricated feedstock filament of composition 90-8-2 ($\times 200$)



(feedstock filament) has been prepared by using different controllable parameters (namely; Temperature, Revolution and Dead weight) and total of 27 (9×3) experiments were conducted to reduce the effect of environmental, human variations etc. According to previous analysis of compositions/ proportion of material it has been concluded that 91-8-1 (PLA-HAp-CS) are mostly/best suitable for fabrication of biocompatible/biodegradable feedstock filament also development of scaffolds on FDM.

Fig. 9 Fabricated feedstock filament of composition 91-8-1 ($\times 400$)

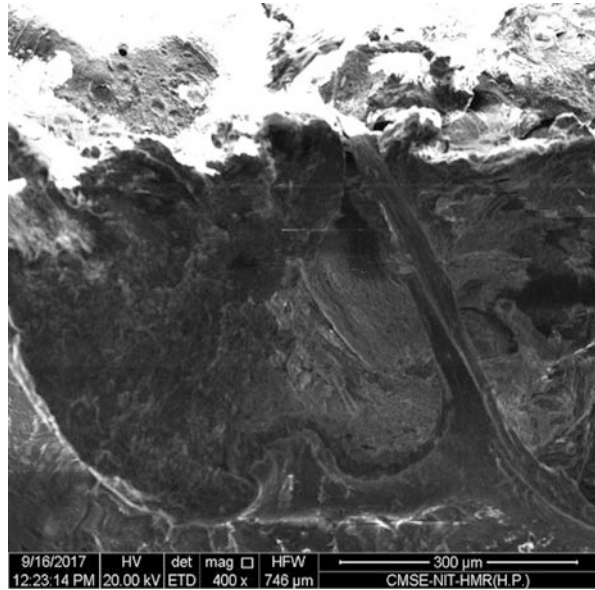
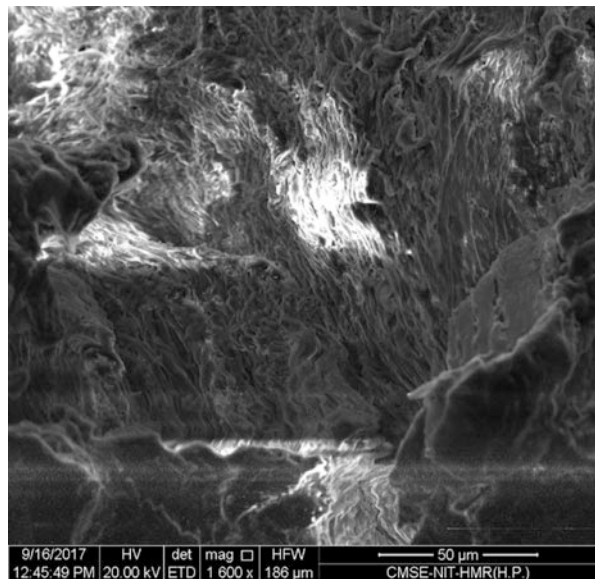


Fig. 10 Fabricated feedstock filament of composition 90-8-2 ($\times 1600$)



7.6 Fabrication of Feedstock Filament Based on DOE

Tensile tests measure the force required to break a materials (polymers/metals) sample specimen and the extent to which the specimen stretches or elongates to that breaking point. Tensile test is the most adoptable test regarding analyse for



Fig. 11 Tensile test using Universal Testing Machine

Table 4 Control log for processing of PLA91-HAp8-CS1

Experiment run no.	Input parameters		
	Temperature ($^{\circ}\text{C}$)	Revolution (rpm)	Dead weight (Kg)
1	170	100	8
2	170	140	10
3	170	180	12
4	180	100	10
5	180	140	12
6	180	180	8
7	190	100	12
8	190	140	8
9	190	180	10

strength of feedstock filament. Tensile testing is to be done on Universal Tensile Tester (UTT) to check the tensile results at break as well as at peak of feedstock filament. Figure 11 shows the universal tensile tester having capacity up to 5000 N, used only for the plastics/polymers material. Polymer feedstock filament, polymer strip or flat of any size can be measured by this UTT.

According to Table 4 (DOE), 9 sets of biocompatible/biodegradable feedstock filament wire has been prepared. Further Table 5 shows outputs of tensile test: Strength at peak (PS), Peak load (PL) and Strength at break (BS) and their Signal

Table 5 Tensile outputs of composition PLA91-HAp8-CS1

Experiment run no.	Output parameters					
	Strength at peak (MPa)	Peak load (N)	Strength at break (MPa)	SNRA 1 (PS)	SNRA2 (PL)	SNRA3 (BS)
1	3.14	6.40	2.83	9.9386	16.1236	9.0357
2	3.64	7.80	3.28	11.2220	17.8419	10.3175
3	4.12	9.00	3.71	12.2979	19.0849	11.3875
4	3.62	7.70	3.22	11.1742	17.7298	10.1571
5	4.25	9.20	3.80	12.5678	19.2758	11.5957
6	3.10	6.30	2.73	9.8272	15.9868	8.7233
7	4.85	10.10	4.38	13.7148	20.0864	12.8295
8	3.76	7.90	3.38	11.5038	17.9525	10.5783
9	4.54	9.50	4.10	13.1411	19.5545	12.2557

Table 6 Analysis of variance for SNRA 1

Source	DF	Adj SS	Adj MS	F-value	P-value	% age contribution
Temperature	2	5.2203	2.61014	36.81	0.026	36.25
Revolution	2	0.0456	0.02280	0.32	0.757	0.32
Dead Weight	2	8.9917	4.49584	63.41	0.016	62.44
Error	2	0.1418	0.07091			0.99
Total	8	14.399				

Table 7 Response table for Signal to Noise Ratios larger is better for SNRA 1

Level	Temperature (T)	Revolution (R)	Dead weight (DW)
1	11.15	11.61	10.42
2	11.19	11.76	11.85
3	12.79	11.76	12.86
Delta	1.63	0.16	2.44
Rank	2	3	1

to Noise (SN) ratio. Based upon Tables 5, 6 and 7 shows percentage contribution of input parameters and their rankings.

As shown in Table 6, percentage error was found to be 0.99%. It shows that model has higher degree of accuracy. Table 7 shows that, dead weight has maximum impact for contributions in SN ratios whereas temperature has minimum contributions.

Further based upon Tables 5, 6, and 7, regression equation for strength at peak has been obtained by using MINITAB software as under:

Regression Equation for Strength at Peak:-

$$\begin{aligned} \text{SNRA1} = & 11.7097 - 0.557 * \text{SNRA_T170} - 0.52 * \text{SNRA_T180} \\ & + 1.077 * \text{SNRA_T190} - 0.101 * \text{SNRA_R100} + 0.055 * \text{SNRA_R140} \\ & + 0.046 * \text{SNRA_R180} - 1.287 * \text{SNRA_DW8} + 0.136 * \text{SNRA_DW10} \\ & + 1.15 * \text{SNRA_DW12} \end{aligned}$$

Here, SNRA_T170, SNRA_T180, SNRA_T190, SNRA_R100, SNRA_R140, SNRA_R180, SNRA_DW8, SNRA_DW10, SNRA_DW12 has been taken from the Table 7, Obtained from Taguchi analysis. After putting the values form the Table 7 in Regression equation final maximized value has been obtained.

$$\begin{aligned} \text{SNRA1} = & 11.7097 - (0.557 * 11.15) - (0.520 * 11.19) + (1.077 * 12.79) - \\ & (0.101 * 11.61) + (0.055 * 11.76) + (0.046 * 11.76) - (1.287 * 10.42) + \\ & (0.136 * 11.85) + (1.150 * 12.86) = 16.620(\text{Predicted value}) \end{aligned}$$

Similarly, for SN ration of strength at peak, final maximized value of the property has been predicted with the help of the following relations.

$$\begin{aligned} \text{SN ratio} = & -10 \log X(\text{standard equation for finding SN ratio}) \\ 16.620 = & -10 \log X \\ X = & 10^{-1.6620} \end{aligned} \tag{1}$$

$$\begin{aligned} X = & 2.1777 * 10^{-2} \text{ now put value of the x in next equation} \\ X = & 1/n \sum 1/y^2 \\ 2.1777 * 10^{-2} = & 1/y^2(\text{here n} = 1) \\ Y^2 = & 1/2.1777 * 10^{-2} \end{aligned} \tag{2}$$

$$Y = 6.776(\text{maximized value of the Strength at Peak})$$

Where, Y is the value of the property.

Similarly, according to SNRA1 calculate value of SNRA2 and SNRA3.
Regression Equation for Peak Load:-

$$\begin{aligned} \text{SNRA 2} = & 18.182 - (0.498 * 17.68) - (0.518 * 17.66) + (1.016 * 19.20) - \\ & (0.202 * 17.98) + (0.175 * 18.36) + (0.027 * 18.21) - (1.494 * 16.69) + \\ & (0.194 * 18.38) + (1.301 * 19.48) = 23.780(\text{Predicted value}) \end{aligned}$$

Y = 15.432 (maximized value of the Peak Load).

Regression Equation for Strength at Break:-

$$\begin{aligned} \text{SNRA 3} = & 10.764 - (0.518 * 10.247) - (0.606 * 10.159) + \\ & (1.123 * 11.888) - (0.090 * 10.674) + (0.066 * 10.830) + (0.024 * 10.789) \\ & - (1.319 * 9.446) + (0.146 * 10.910) + (1.173 * 11.938) = 15.80(\text{Predicted value}) \end{aligned}$$

Y = 6.166 (maximized value of the Strength at Break)

Based upon Tables 5, 6, 7, 8, and 9 respectively shows the response optimization and best settings predicted from multi factor optimization point of view. The same has been reflected in Fig. 12 as optimization plot, which clearly states that temperature at 190 °C, RPM 140 and dead weight 12 kg are the optimized settings.

Table 8 Response optimization: SNRA3, SNRA2, and SNRA1

Response	Goal	Lower	Target	Upper weight	Importance
SNRA3	Maximum	8.7233	12.8295	1	1
SNRA2	Maximum	15.9868	20.0864	1	1
SNRA1	Maximum	9.8272	13.7148	1	1

Table 9 Best setting obtained with best Signal to Noise Ratios

Solution	Temperature	Revolution	Dead weight	SNRA3 fit	SNRA2 fit	SNRA1 fit	Composite desirability
1	190	140	12	13.1269	20.6733	13.9918	1

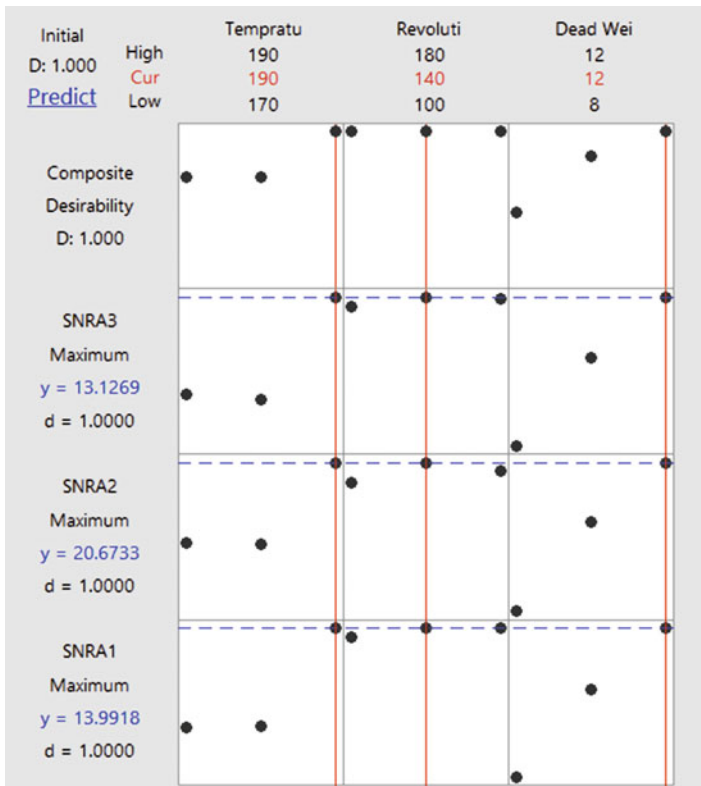


Fig. 12 Optimization plot of tensile test using UTT

8 Summary

In this study, PLA, HAp and CS based composite material has been used for fabrication of biocompatible and biodegradable feedstock filament. Following are the conclusions from the present study:

- (a) In MFI testing (according to Table 1) of different compositions it was found that only four composition (84%–4%–12%, 80%–8%–12%, 91%–8%–1%, 90%–8%–2%) flow rate is continuous which is suitable for drawing the feedstock filament.
- (b) The peak strength according to Table 2, two compositions/proportion (91%–8%–1%, 90%–8%–2%) is high which is highly suitable to work on FDM for preparation of scaffolds.
- (c) In thermal analysis it was concluded that; according to Fig. 6 and Table 3 two compositions (91%–8%–1% and 80%–8%–12%) are less crystallization, which is best suitable for using biomedical applications/implants other compositions are more crystalline.
- (d) Based upon SEM analysis (Figs. 7, 8, 9, and 10) concluded that both the compositions/ proportions (91%–8%–1% & 90%–8%–2%) of feedstock filament grain structure is similar to open porous structure. Hence can be gainfully employed for cell growth.
- (e) Overall, based on rheological, Thermal and Tensile experimentation it has to conclude that best composition for working on TSE, FDM and for biomedical applications/ implants is “PLA91%-HAp8%-CS1%” because it has continuous and good flowability, high tensile strength (Peak strength), suitable glass transition and melting temperature and also low crystalline; which has suitable for biomedical applications.
- (f) Finally based upon Taguchi analysis and regression model for PLA91%-HAp8%-CS1% based feed stock filament, temperature at 190 °C, RPM 140 and dead weight 12 kg are the recommended optimized settings on TSE. The functional prototypes developed at proposed settings will have better scaffolding which will provides attractive surfaces for new bone cells.

Acknowledgements The authors are thankful to SERB (DST), GOI for financial support and Manufacturing Research Lab (Dept. of Production Engineering, Guru Nanak Dev Engineering College, Ludhiana), Punjabi University Patiala for technical support.

References

1. Anitha, R. and Arunachalam, S. (2001), “Critical parameters influencing the quality of prototypes in fused deposition modeling”, *Journal of Materials Processing Technology*, Vol. 113, Issue 1–3, pp. 385–388.
2. Chhabra, M. and Singh, R. (2011), “Rapid casting solutions a review”, *Rapid Prototyping Journal*, Vol. 17, pp. 328–350.
3. Choudhury, A., Chakraborty, D. and Reddy, B. (2007), “Extruder path generation for Curved Layer Fused Deposition Modeling”, *Computer-aided design Journal*, Vol. 40, pp. 235–243.
4. Singh, R., Singh, S., Singh, I. P., Fabbrocino, F. and Fraternali, F. (2017), “Investigation for surface finish improvement of FDM parts by vapour smoothing process”, *Composites Part B: Engineering*, Vol. 111, pp. 228–234.
5. Kumar, R., Singh, R., Hui, D., Feo, L. and Fraternali, F. (2017), “Graphene as biomedical sensing element: State of art review and potential engineering applications”, *Composites Part B: Engineering*, <https://doi.org/10.1016/j.compositesb.2017.09.049>

6. Singh, R., Kumar, R., Feo, L. and Fraternali, F. (2016), "Friction welding of dissimilar plastic/polymer materials with metal powder reinforcement for engineering applications", *Composites Part B: Engineering*, Vol. 101, pp. 77–86.
7. Block, J. E. and Poser, J. (1995), "Does xenogeneic demineralized bone matrix have clinical utility as a bone graft substitute?", *Med Hypotheses*, Vol. 45, pp. 27–32.
8. Sasso, R. C., Williams, J. I., Dimasi, N., Meyer Jr. P. R. (1998), "Postoperative drains at the donor site of iliac-crest bone grafts. A prospective, randomized study of morbidity at the donor site in patients who had a traumatic injury of the spine", *J Bone Joint Surgical Am*, Vol. 80, pp. 631–635.
9. Rose, F. R. A. J. and Oreffo, R. O. C. (2002), "Bone tissue engineering: hope vs hype", *BiochemBiophys Res Commun*, Vol. 292, pp. 1–7.
10. Du, C., Cui, F. Z., Zhang, W., Feng, Q. L., Zhu, X. D. and Groot, K. D. (2000), "Formation of calcium phosphate/collagen composites through mineralization of collagen matrix", *J Biomed Mater Res A*, Vol. 50, pp. 518–27.
11. Kikuchi, M., Itoh, S., Ichinose, S., Shinomiya, K. and Tanaka, J. (2001), "Self organization mechanism in a bone-like hydroxyapatite/collagen nanocomposite synthesized in vitro and its biological reaction in vivo", *Biomaterials*, Vol. 22, pp. 1705–11.
12. Burg, K. J. L., Porter, S. and Kellam, J. F. (2000), "Biomaterial developments for bone tissue engineering", *Biomaterials*, Vol. 21, pp. 2347–2359.
13. Chang, M. C. and Tanaka, J. (2002), "XPS study for the microstructure development of hydroxyapatite-collagen nano-composites cross linked using glutaraldehyde", *Biomaterials*, Vol. 23, pp. 3879–85.
14. Grodzinski, J. J. (1999), "Biomedical application of functional polymers", *React Function Polymer*, Vol. 39, pp. 99–138.
15. Hutmacher, D. W. (2000), "Scaffolds in tissue engineering bone and cartilage", *Biomaterials*, Vol. 21, pp. 29–43.
16. Ishihara, M., Ono, K., Saito, Y., Yura, H., Hattori, H. and Matsui, T. (2001), "Photo cross-linkable chitosan: an effective adhesive with surgical applications", *Int Cong Ser*, Vol. 1223, pp. 251–257.
17. Madihally, S. V. and Matthew, H. W. T. (1999), "Porous chitosan scaffolds for tissue engineering", *Biomaterials*, Vol. 20, pp. 1133–1142.
18. Mi, F. L., Tan, Y. C., Liang, H. F. and Sung, H. W. (2002), "In vivo biocompatibility and degradability of a novel injectable-chitosan-based implant", *Biomaterials*, Vol. 23, pp. 181–91.
19. Wang, L. S., Khor, E., Wee, A. and Lim, L. Y. (2002), "Chitosan-alginate PEC membrane as a wound dressing: assessment of incisional wound healing", *J Biomed Mater Res B*, Vol. 63, pp. 610–618.
20. Li, Z. S., Ramay, H. R., Hauch, K. D., Xiao, D. M. and Zhang, M. Q. (2005), "Chitosan-alginate hybrid scaffolds for bone tissue engineering", *Biomaterials*, Vol. 26, pp. 3919–3928.
21. Sarasam, A. and Madihally, S. V. (2005), "Characterization of chitosan-polycaprolactone blends for tissue engineering applications", *Biomaterials*, Vol. 26, Issue 5, pp. 500–508.
22. Shanmugasundaram, N., Ravichandran, P., Reddy, P. N., Ramamurty, N., Pal, S. and Rao, K. P. (2001), "Collagen-chitosan polymeric scaffolds for the in vitro culture of human epidermoid carcinoma cells", *Biomaterials*, Vol. 22, pp. 1943–1951.
23. Andrew, C. A. W., Eugene, K. and Garth, W. H. (1998), "Preparation of a chitin-apatite composite by in situ precipitation onto porous chitin scaffolds", *J Biomed Mater Res A*, Vol. 41, pp. 541–548.
24. Kawakami, T., Antoh, M., Hasegawa, H., Yamaguchi, T., Ito, M. and Eda, S. (1992), "Experimental study on osteoconductive properties of chitosan-bonded hydroxyapatite self-hardening paste", *Biomaterials*, Vol. 13, pp. 759–763.
25. Yamaguchi, I., Tokuchi, K., Fukuzaki, H., Koyama, Y., Takakuda, K. and Monma, H. (2001), "Preparation and microstructure analysis of chitosan/hydroxyapatite nanocomposites", *J Biomed Mater Res A*, Vol. 55, pp. 20–27.

26. Yin, Y. J., Zhao, F., Song, X. F., Yao, K. D., Lu, W. W. and Leong, J. C. (2000), "Preparation and characterization of hydroxyapatite/chitosan-gelatin network composite", *J Appl Polym Sci*, Vol. 77, pp. 2929–2938.
27. Ariyapitipun, T., Mustapha, A. and Clarke, A. D. (1999), "Microbial shelf life determination of vacuum-packaged fresh beef treated with polylactic acid, lactic acid, and nisin solutions", *Journal of food protection*, Vol. 62, Issue 8, pp. 913–920.
28. Kale, G., Auras, R., Singh, S. P. and Narayan, R. (2007), "Biodegradability of polylactide bottles in real and simulated composting conditions", *Polymer Testing*, Vol. 26, Issue 8, pp. 1049–1061.
29. Fini, M., Giannini, S., Gioradano, R., Giavaresi, G., Grimaldi, M. and Aldini, N. N. (1995), "Resorbable device for fracture fixation: in vivo degradation and mechanical behavior", *Int J Artif Organs*, Vol. 18, pp. 772–776.
30. Shen, X. Y., Tong, H., Jiang, T., Zhu, Z. H., Wan, P. and Hu, J. M. (2007), "Homogeneous chitosan/carbonate apatite/citric acid nano-composites prepared through a novel in situ precipitation method", *Compos Sci Technology*, Vol. 67, pp. 2238–2245.
31. Taddei, P., Monti, P. and Simoni, R. (2002), "Vibrational and thermal study on the in vitro and in vivo degradation of a poly (lactic acid) based bio-absorbable periodontal membrane", *J Mater Sci Mater Med*, Vol. 13, pp. 469–475.
32. Shen, X. Y., Tong, H., Zhu, Z. H., Wan, P. and Hu, J. M. (2007), "A novel approach of homogenous inorganic/organic composites through in situ precipitation in poly-acrylic acid gel", *Mater Lett*, Vol. 61, pp. 629–634.
33. Gupta, B., Revagade, N. and Hilborn J. (2007), "Poly (lactic acid) fiber: an overview", *Prog. Polym.Sci.*, Vol. 32, pp. 455–482.
34. Ge, Z., Goh, J.C., Wang, L., Tan, E.P. and Lee, E.H. (2005), "Characterization of knitted polymeric scaffolds for potential use in ligament tissue engineering", *J. Biomater. Sci. Polym. Ed.*, Vol. 16, pp. 1179–1192.
35. Ouyang, H.W., Goh, J.C., Thambyah, A., Teoh, S.H. and Lee, E.H. (2003), "Knitted polylactide-co-glycolide scaffold loaded with bone marrow stromal cells in repair and regeneration of rabbit Achilles tendon", *Tissue Eng.*, Vol. 9, pp. 431–439.
36. Freeman, J.W., Woods, M.D. and Laurencin, C.T. (2007), "Tissue engineering of the anterior cruciate ligament using a braid-twist scaffold design", *J. Biomech.*, Vol. 40, pp. 2029–2036.
37. Singh, R., Kumar, N., Ranjan, N., Penna, R. and Fraternali, F. (2017), "On the recyclability of polyamide for sustainable composite structures in civil engineering", *Composite Structures*, <https://doi.org/10.1016/j.compstruct.2017.10.036>
38. Kalita, S.J., Bhardwaj, A. and Bhatt, H.A. (2007), "Nanocrystalline calcium phosphate ceramics in biomedical engineering", *Material Science and Engineering: C*, Vol. 27, Issue 3, pp. 441–449.
39. Mostafa, N.Y. and Brown, P.W. (2007), "Computer simulation of stoichiometric hydroxyapatite: Structure and substitutions", *Journal of Physics and Chemistry of Solids*, Vol. 68, Issue 3, pp. 431–437.
40. Teixeira, S., Rodriguez, M.A., Pena, P., De Aza, A.H., De Aza, S. and Ferraz, M.P. (2009), "Physical characterization of hydroxyapatite porous scaffolds for tissue engineering", *Material Science and Engineering: C*, Vol. 29, Issue 5, pp. 1510–1524.
41. Guo, L., Huang, M. and Zhang, X. (2003), "Effects of sintering temperature on structure of hydroxyapatite studied with Rietveld method", *Journal of Materials Science: Material in Medicine*, Vol. 14, Issue 9, pp. 817–822.
42. Auras, R., Harte, B. and Selke S. (2004), "An overview of polylactides as packaging materials", *Macromol. Biosci.*, Vol. 4, pp. 835–864.
43. Ravindra, R., Krovvidi, K.R. and Khan, A.A. (1998), "Solubility parameter of chitin and chitosan", *Carbohydr. Polym.*, Vol. 36, pp. 121–127.
44. Bonilla, J., Fortunati, E., Vargas, M., Chiralt, A. and Kenny, J.M. (2013), "Effects of chitosan on the physicochemical and antimicrobial properties of PLA films", *J. Food Eng.*, Vol. 119, pp. 236–243.